Climate Warming and Effects on Aviation

Diandong Ren and Lance M. Leslie

Abstract

The greatest concerns of the aviation industry under a warming climate possibly are the following two questions: first, what are the consequences for maximum payloads? and second, will changed air properties (density, temperature and viscosity) affect fuel efficiency? Here, the effects of climate warming on maximum payload and fuel efficiency are examined using atmospheric parameters from 27 climate models. Historical (20th century) climate simulations credibly reproduce the reanalysis period (1950–2015) of near-surface air density (NSAD). Lower NSAD is a first-order global signal continuing into the future. The NSAD reduction impact on MTOW could be ~1% over the busy North Atlantic Corridor (NAC), and also varies among aircraft. Furthermore, for the standard 7-stage flight profile, negative effects of warming on fuel efficiency affect civil aviation. The cruising stage consumes most aviation fuel, and as cruising altitude coincides with the tropopause, the tropopause structure in a warming climate supports the conclusions drawn here. Tropopause temperature changes cause only ~0.08% reduction in thermal efficiency. The net effect on total efficiency is smaller because of improved mechanical efficiency. Work required for a commercial aircraft increases in a warmer climate due to elevated tropopause altitude and increased air drag. The latter outweigh the former by almost an order of magnitude, for international flights.

Keywords: tropopause, civil aviation industry, climate warming, aircraft payload, fuel efficiency, GCMs, climate change adaptation

1. Introduction

Aviation is probably the most reliable means of disaster response and relief for most large-scale natural disasters. For example, it is unrealistic to maintain or repair road or rail connections across areas affected by earthquakes, floods, landslides, storms, or wildfires, to transport relief and aid to those affected. Thus, adaptation and risk management must pay particular attention to the strengthening of aviation infrastructure to guarantee robust and sustainable relief. By providing a perspective on the impacts on aviation of anticipated changed atmospheric conditions over the near future, this research addresses the adaptation of aviation transport to climate change. The greatest concerns of the aviation industry under a warming climate possibly are the following two questions: how will the maximum payload be affected by the warmer and lighter lower layer atmosphere? and, during the journey, will the changed ambient air properties (density, temperature and viscosity) affect the engine performance? Anyway, all current aviation engines are breathing

thermal engines. The first part of this chapter focuses on the maximum payload, whereas the second part concentrates on the effects on the efficiency and fuel consumption of the thermal engines. Commercial airliners provide an environment-friendly express means of cargo transport and personnel travel (Section 7.4.1.2 of IPCC AR5 [1]). Possible effects of aviation on atmospheric components and climate already have been studied in detail [2–7]. Conversely, the the effects of climate warming on aviation have not yet been extensively studied. In Section 1 of this chapter, climate warming effects on aviation payload are investigated, based on the fact that air density is proportional to the maximum take-off weight (MTOW) for an aircraft, irrespective of the design (fixed wing or helicopters; jets or propellers). Aircraft are air-lifted and the MTOW can be expressed in a generic form as

$$MTOW = M\rho_a \left| \vec{V_0} \right|^2, \tag{1}$$

where M is airplane mechanical properties such as wing span area, attack angle, and fuselage-wing interaction, ρ_a is air density, and $\vec{V_0}$ is aircraft taking-off speed (for helicopters and other rotorcrafts, the angular speed of the rotor blades). If taking-off speed also is deemed as aircraft property, then air density is the sole environmental factor that is directly proportional to $MTOW$. In this study, near-surface (airport elevation) air density variations are examined over the twentieth and twenty-first centuries. For period with reanalysis data (1950–present), the loyalty of air density simulated by 27 climate models (**Table 1**) to reality also is examined. Based on the analyses, the decrease of maximum payload is examined, and the inter-model spread of the uncertainty assessed up to 2100. The largest uncertainty in the degree of warming resides with the industrial emission of GHGs and other pollutants in the atmosphere to which climate is sensitive to the extra radiative forcing, because modern climate has a clear footprint of human activity [2, 8]. The future state of climate would depend crucially on what emission controls nations chose to impose. Emission scenarios (ESs) describe future release into the atmosphere of GHGs, aerosols, and other pollutants. ESs and other boundary conditions are inputs to climate models. In the most recent Intergovernmental Panel on Climate Change (IPCC) assessment report (AR5), the driving scenario is in the form of representative concentration pathways (RCPs). In this study, the climate model outputs under high scenario RCP 8.5 (meaning that rising radiative forcing pathway leads to 8.5 W/m^2 heating effects in 2100) are used.

The second theme of this chapter is on aviation fuel efficiency. According to FAA regulations, the flight profile consists the seven stages (A-G from taxi out till taxi in). To estimate the extra work that needs to be performed, along flight route integration is the exact approach. Because the commercial data on flight logs are not available for us, we have to make some assumptions according to the carrier aircraft and the routes, which are readily available online (e.g., from those websites selling air tickets). Unlike the issue with maximum payload, where only the airport level air density plays the decisive role, temperature, air density, and winds all matter in the fuel efficiency issue. There sure exist apparent canceling effects among them as well. In addition, the tropopause's elevation will fluctuate as climate warms; this involves extra potential energy cost in case the aircraft still cruise in the coldest (hence the most favorable for the thermal engine) and most clear level of the Earth's atmosphere. This likely is the case since the cruise stage is the most fuel-consuming stage of the flight (although the rate of fuel burning is only a half of

Model Name	Institution	Horizontal resolution
ACCESS1-0	Commonwealth Scientific and Industrial Research Organization (CSIRO)/Bureau of Meteorology (BoM)	192×145
ACCESS1-3	CSIRO/BoM	192×145
CCSM4	National Center for Atmospheric Research	288×192
CanESM2	Canadian Center for Climate Modelling and Analysis	128×64
CNRM-CM5	Centre National de Recherches Meteorologiques	256×128
CESM1-BGC	National Center for Atmospheric Research	288×192
CESM1-CAM5	National Center for Atmospheric Research	288×192
FGOALS-g2	Institute of Atmospheric Physics, Chinese Academy of Sciences	128×60
GFDL-CM3	Geophysical Fluid Dynamics Laboratory	144×90
GFDL-ESM-2G	Geophysical Fluid Dynamics Laboratory	144×90
GFDL-ESM-2M	Geophysical Fluid Dynamics Laboratory	144×90
GISS-E2-H	NASA/Goddard Institute for Space Studies (GISS)	144×90
GISS-E2-R	NASA/GISS	144×90
HadGEM2_AO	National Institute of Meteorological Research, Korea Meteorological Administration (S. Korea)	192×145
HadGEM2_CC	Met Office Hadley Centre	192×145
HadGEM2_ES	Met Office Hadley Centre	192×145
INM	Institute of Numerical mathematics, Russian Academy of Sciences	180×120
IPSL-CM5A-LR	Institut Pierre Simon Laplace (France)	96×96
IPSL-CM5A-MR	Institut Pierre Simon Laplace (France)	144×143
IPSL-CM5B-LR	Institut Pierre Simon Laplace (France)	96×96
MIROC5	Atmosphere and Ocean Research Institute, The Tokyo University	256×128
MIROC-ESM	Japan Agency for Marine-Earth Science and Technology	128×64
MRI-CGCM3	Meteorological Research Institute	320×160
MPI-ESM-LR	Max Plank Institute (MPI) for Meteorology	128×64
MPI-ESM-MR	Max Plank Institute (MPI) for Meteorology	192×96
NorESM1-M	Bjerknes Center for Climate research, Norwegian Meteorological Institute	144×96
NorESM1-ME		144×96 global grids

Table 1.
Twenty-seven GCM models used in this study.

the ascending stage). So, a complete consideration of the issue involves the along flight route integration plus the potential energy changes of the entire aircraft. Discussion bifurcates in the following sections, focusing, respectively, on the effects on maximum payload (Section 2) and fuel efficiency (Section 3). This study should inspire further investigation into how climate and environmental changes influence the civil aviation sector of industry.

2. Adverse effects on maximum payload from a warmer climate

2.1 Methods and data

Air density is derivable from air pressure, temperature, and humidity [9, 10]:

$$\rho_a = P/[R_d T(1 + 0.608q)] \qquad (2)$$

where P is air pressure (Pa), R_d is dry air gas constant ($\sim$287 J/kg/K), T is absolute air temperature (K), and q is specific humidity (g/g). To apply Eq. (2) to near-surface level, atmospheric fields of pressure (Ps), temperature (Ts), and specific humidity qs at ground level (subscript "s" means surface) are required. These parameters fortunately are primary outputs from the coupled model intercomparison project (CMIP, e.g., https://cmip.ucar.edu/; Ref. [11]). The monthly climate model outputs are obtained from the IPCC Deutsches

Klimarechenzentrum (DKRZ) Data Distribution Centre (http://www.ipcc-data.org/sim/gcm_monthly/AR5/Reference-Archive.html). For models providing multiple perturbation runs, only *r1i1p1* runs are used. To examine whether the historical runs from the climate models are close to reality in their simulated air density, NCEP/NCAR reanalyses are used as observations. The monthly NCEP/NCAR reanalysis [12] data are obtained from the Earth System Research Laboratory website: http://www.esrl.noaa.gov/psd/data/gridded/data.ncep.reanalysis.pressure.html. Specific humidity provided by reanalyses can be converted into specific humidity before applying Eq. (2).

2.2 Results and discussion

From Eq. (2), two factors cause air density fluctuations: temperature changes and mixing in tracers of different molecular weight to the average molecular weight of the air. Earth atmosphere is dominated by the "dry" inactive components (N_2, O_2, CO_2, etc.). With heat intake, the primary response is expanding in volume and, subsequently, an increased mass center. During the past half century, on average, there is a 30 m lift of the mass center, indicating that the mass is now distributed in a thicker (larger depth) layer (thus reduced density at lower levels). Heating caused expansion is just one effective means that decreases air density throughout the entire tropospheric atmosphere. In-taking of lighter molecules
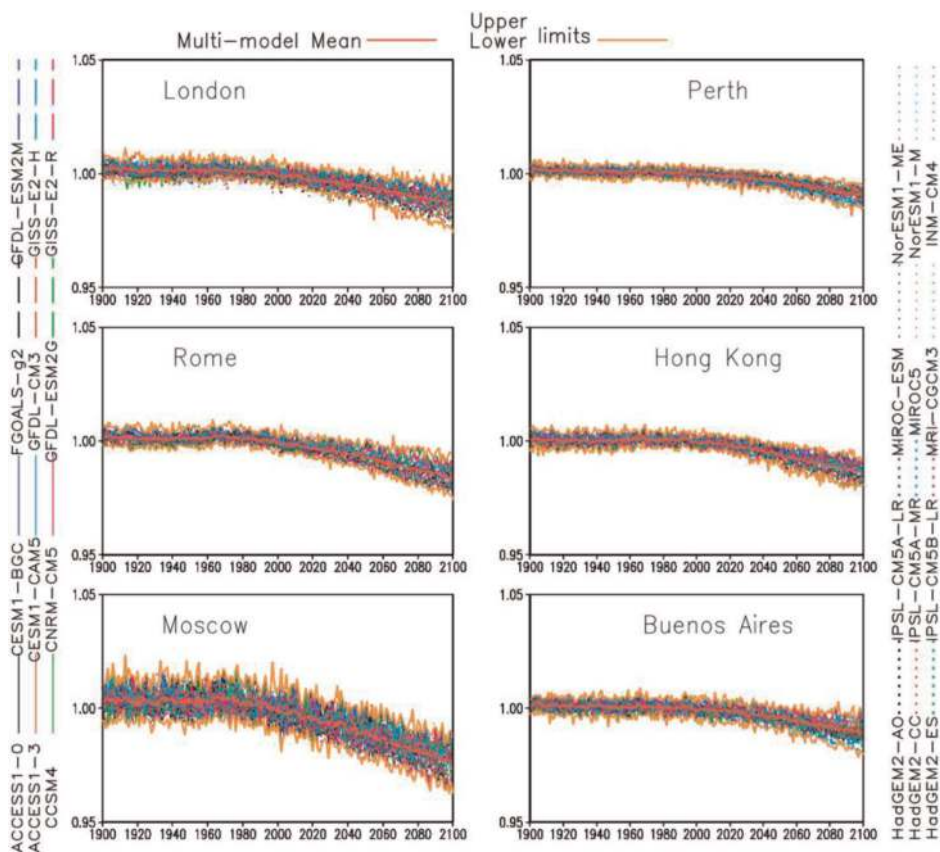

Figure 1.
Changes in near-surface air density for the period 1900–2100 as simulated by 24 climate models over six selected world airports. Near-surface air density estimated from NCEP/NCAR reanalyses is shown as red bold lines. The upper and lower bounds among the 24 climate models are shown as brown lines. The analyses were performed on monthly data and averaged to annual values (actual plotted). As with all land-ocean-ice sheet fully coupled climate model outputs, the exact timing is hard to pinpoint. Only the statistical properties and long-term averages would resemble reality.

(H_2O has smaller molar mass than N_2 and O_2, the dominant constituents of dry air) is another effective way of reducing air density. Although from Clausius-Clapeyron equation [13] warm air has more capacity of holding moisture, it still is debatable whether earth atmosphere actually gains mass, because the hydrological cycle also tends to intensify [14–16], through facilitating interhemispherical moisture exchange [17] and destabilizing local stratification profile [15, 16]. If precipitation increases more than evaporation, there still is a net mass loss for atmosphere. Interestingly, all existing reanalysis datasets show no statistically significant changes in global total air mass during their respective reanalyses period. This implies that the net water vapor input into atmosphere is globally delicately balanced between geographic regions.

Applying the formula as in Eq. (2) to climate model-simulated (under RCP 8.5, a strong emission scenario) near-surface pressure, temperature, and humidity, near-surface air density is estimated over the globe. The same formula also is used on the NCEP/NCAR reanalysis data. Density variations over 1900–2100 for six global airports are shown in **Figure 1**, as representatives. All 27 climate models unanimously indicate that all six locations experienced salient density decreases. Significant inter-model spread exists but started well before the year 1900 and should be ascribed to model systematic biases/drifts. For each climate model, the amount of density decrease easily exceeds the natural interannual variability magnitude. Geographically, high-latitude regions (e.g., Moscow) have larger
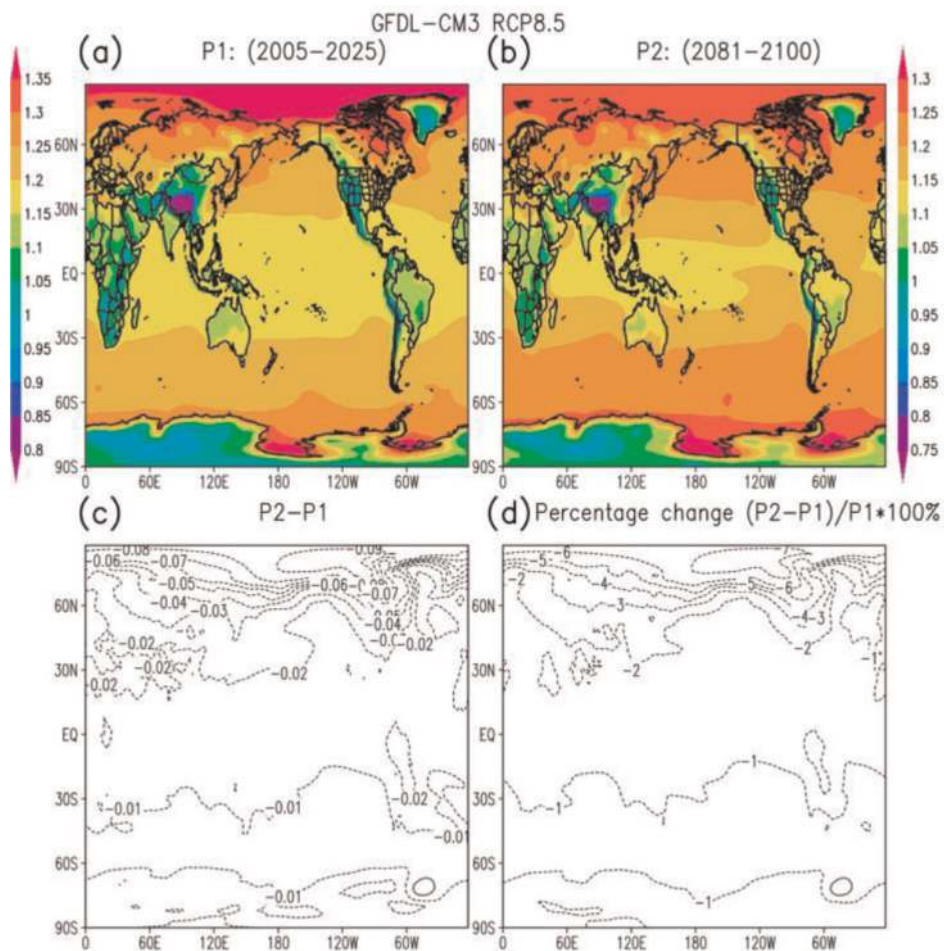

Figure 2.
GFDL-CM3-simulated near-surface air density (kg/m³) averaged over two periods: (2005–2025) (a) and (2081–2100) (b), under RCP 8.5 scenario assumption. The density differences between these two periods are shown in (c), with corresponding percentage changes shown in (d).

interannual density variability but also generally experiences larger density decreases over the simulated 200 years. The linear trends of decrease estimated based on the reanalyses are close to model simulation. All 27 climate models show high degree of consensus in the simulated air density changes (e.g., **Figure 2** for GFDL-CM3).

Air density changes are a gradual process over the years. To quantitatively examine if the density changes were statistically significant, a *t*-test was performed over the two 20-year annual density time series (2005–2025 and 2081–2100). In **Figure 3**, the *t*-value (right panels) and corresponding *P*-values (left panels, for a DoF of 38) are presented (six climate models are shown to demonstrate this). Under the RCP 8.5 scenario, most global regions pass the 95% confidence interval. The signal-to-noise ratio is low only for very limited oceanic regions off the southern tip of Greenland and some sectors of the Southern Ocean. The oceanic region off southern Greenland collocates with the deep-water formation region of the North Atlantic meridional overturning circulation (MOC). Further investigation indicates that the lack of a decrease in density is due to a weakened MOC that places less moisture into the atmosphere. Regionally, the air becomes drier and heavier. On the other hand, warming reduces the air density. These two canceling factors make the net reduction in density statistically insignificant or, when the moistening effect wins out, may even increase the air density. For this study, the oceanic regions that
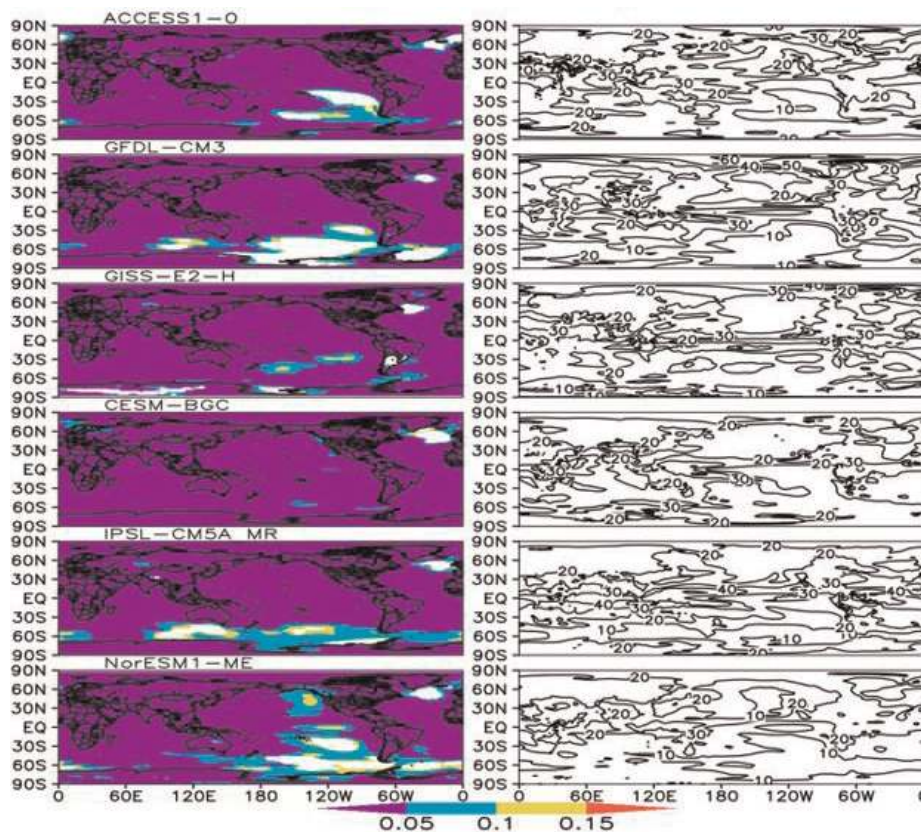

Figure 3.
A t-test was performed for near-surface air density (simulated under RCP 8.5 scenario) annual time series over two periods (2005–2025) and (2080–2100). Sophisticated modern climate models show consensus on the geographical patterns of the P-value (left panels) and t-values (right panels). Except for some oceanic regions off the southern tip of Greenland and some portions of the Southern Oceans, most global regions passed the 95% confidence interval, for a DoF of 38. Tropical regions, especially over the intertropical convergence zone (ITCZ), experienced the most significant density decreases. The oceanic region off southern Greenland collocates with the region of deep-water formation of the North Atlantic meridional overturning circulation (MOC).

did not pass the *t*-test can be disregarded, because a very limited number of airports are marine-based. Unlike the percentage changes, the tropical region, especially the intertropical convergence zone (ITCZ, an area of low pressure and convergence of trade winds), had the lowest *P*-value, meaning that the changes over the region are most likely to be statistically significant. From Eq. (2), air density is co-controlled by temperature change and vapor content change. The temperature changes over tropical regions are smaller than over the high-latitude regions. What make the changes over tropical regions statistically more significant are the relatively small changes in air density, for all time scales.

Although air density values simulated by the 27 climate models, when compared with those derived from the NCEP/NCAR reanalysis data, have systematic biases, the linear trends derived from models agree very well with the reanalyses. This indicates that for estimating payload decreases as the climate warms, the density time series can be normalized by their average value over a control period, say 1900–1920. For a specific model, differences in the values of the normalized density time series from unity are the percentage reductions of NSAD and MTOW. If one further assumes an invariant unavoidable load (weight of an empty airplane), the decrease of MTOW also is the decrease of maximum payload. Air density changes estimated from all climate models were interpolated to the same spatial resolution as MRI-CGCM3. **Figure 4** shows the MTOW changes between the two 20-year periods (2005–2025 and 2080–2100). Globally, the changes can reach 5% reduction for some high-latitude and high-elevation airports. For the busy North Atlantic Corridor (NAC), the reduction generally is greater than 1%. This has important economic significance. For the Boeing 747-400, this means a net load reduction of about 3969 kg (**Table 2**), approximately the passenger and luggage weight of ~25 passengers, or a ~6% reduction in its full passenger carrying capacity. Actual payload equivalence of a 1% reduction in MTOW for other types of aircraft is listed in **Table 2**. Because the ratio of unavoidable load to its maximum effective payload varies for different aircraft, the general reduction in net payload over NAC varies from 5 to 8.3% for all the aircraft types considered. Some Northern Hemisphere
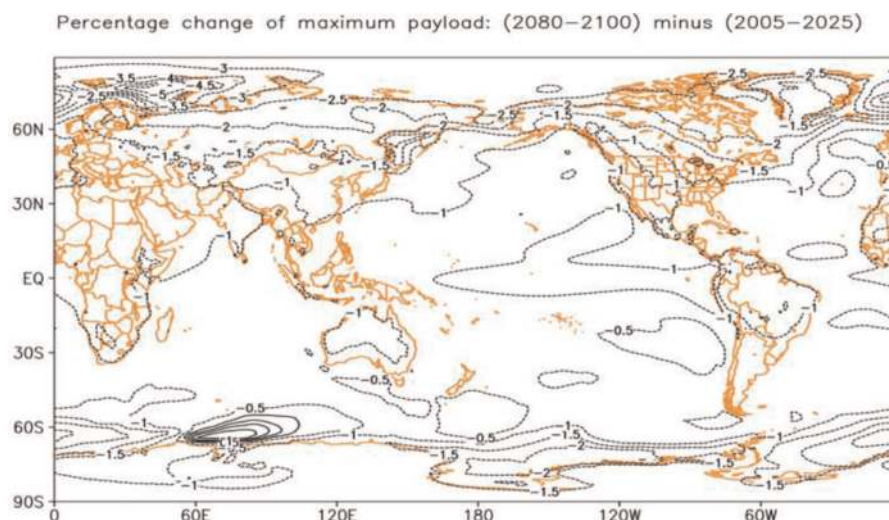

Figure 4.
The estimated ensemble mean decrease in aircraft maximum takeoff total weight (MTOW), as a percentage, based on air density changes simulated by 27 climate models under the RCP 8.5 scenario. The near-surface density from each climate model was normalized by its mean value over 2005–2025 (the control period). Then a bilinear interpolation scheme was used to interpolate on to MRI-CGCM3's horizontal resolution. An ensemble average was taken over the climate models. The reduction can reach 5% over Northern Europe. For the North Atlantic Corridor (NAC), a ~1% reduction in MTOW was reached during the 75-year span.

Aircraft Type	1% MTOW [kg]	Aircraft Type	1% MTOW [kg]	Aircraft Type	1% MTOW [kg]	Aircraft Type
Bombardier (Bom) CS300	653.2	Antonov An-124-100M	4050.6(1.7%)	Douglas DC-8-61	1474.2	McDonnell Douglas MD-90 30
Vickers Viscount 800	303.9(3%)	Lockheed L-1011-200	2113.7	Handley Page Hermes	390.1	de Havilland (dH Comet 1
Airbus A330-200	2300(1.97%)	B767-400ER	2041.2	B727-100	771.1	Bom CS100
Tupolev Tu-154M	1043.3	Bom CRJ700	329.8	MD-83 (2.2%)	725.7	Ilyushin IL-96-30
A380-800	5443.1(1.9%)	Boeing 787-8	2279.3	B707-120B	1165.7	A318
Boeing B747-8	4477.0(2%)	A350-1000	3079.9	B707-320B	1513.2	B737-600
B747-400ER	4127.7	IL-86	2079.7	B720B	1061.4	B737-400
B747-400	3968.9	B767-300ER	1868.8	B727-200	838.2	B737-300
B747-200	3778.4	A300-600R	1719.1	HS Trident 2E	646.4	B717-200HGW
B747-300	3778.4	A300-600[7]	1632.9	Caravelle III	459.9	B737-500
A340-200	2535.1	B737-900ER	851.4	DC-6B	485.3	Embraer ERJ 145
A340-500	3719.5	A310-300[7]	1569.9	dH Comet 2	544.3	Embraer 190
B777-200LR	3474.5	A310-200	1416.4	Convair 880	875.4	Embraer 175
B747-100	3333.9	A400M	1409.8	ATR 42-500	186.0	Embraer 170
B777-300	2993.7	B757-300	1236.0	ATR 72-600	227.7	Bom CRJ900
MD-11	2732.9	B757-200	1156.7	DC-4	331.1	Bom Q400
Il-96M	2698.9	Tu-204SM	1043.3	DC-6	440.9	Saab 2000
A350-900	2680.7	A321-100	829.6	DC-6A	486.3	Bom CRJ200
A340-600	3674.1	the Concorde	1850.7	dH Comet 3	680.4	B717-200BGW
B777-300ER	3515.3	B767-300	1587.6	dH Comet 4	707.6	Fokker 100
B777F	3478.1	Vickers VC10	1518.6	dH Hercules	70.8	Avro RJ-85
B777-200	2472.1	B737-700	851.4	DC-7	553.4	A330-300
A350-800	2590.0	B737-800	790.2	DC-8-32	1406.1	B737-700
A340-300	2766.9	A319	640.0	DC-8-51	1251.9	An-225
B787-9	2508.4	A320-100	679.9	A380-800F	5896.7	B377

Table 2.
Actual payload equivalence of a 1% reduction in near-surface air density (NSAD). Percentages of maximum payload equivalence are shown in parenthesis.

high latitudes have a ~5% decrease in NSAD or MTOW. Considering that a 1% reduction in MTOW corresponds to a ~2% (for larger aircraft such as a Boeing 747-800 or an An-24) to ~3.6% (for small aircrafts such as an Embraer ERJ-145) reduction in effective payload, the ~5% reduction in MTOW means a ~8.5–19% reduction in effective payload year-round. As we stated earlier, at the costs of extra maintenance, aircraft still can operate with the manufacturer-labeled MTOW, which is lower than MTOW, under the unfavorable condition of warming. There may be no apparent passenger or cargo reduction. However, there will be hidden extra costs from a warming atmosphere.

2.3 Discussion

Based on the diagnosis of stresses (and forces) exerted on aircraft, a suitable invariant entity was identified for investigating climate change effects on aviation payload. Assuming no changes in technical aspects of aircraft and no changes to FAA regulations on takeoff performance, near-surface air density is the single most significant atmospheric parameter. Reanalyses data indicated clearly that the Earth's atmosphere had expanded in volume in the past half century.

Consequently, the near-surface air density experienced significant decreases globally. The 27 climate models showed a high level of consensus in simulated near-surface air density variations. The ensemble mean of their twenty-first century simulations in NSAD trends was used to examine future reduction to effective payload. In line with Ref. [18], our study aimed to illustrate the potential for rising temperatures to influence weight restriction at takeoff stage. All technical aspects as commented on by Ref. [19] were assumed to be invariants during the analyses period. The simple fact that during extreme hot weather in summertime cargo airplanes have to reduce the effective payload indicates the validity of such analyses. The difference found with seasonal cycle is that these superimposed effects

work persistently year-round and there is no easy way to circumvent or ameliorate them. We, however, agree with Ref. [19] that aviation industry still has technical room to cope with the detrimental effects from climate warming, perhaps at the extra costs of maintenance, passenger comfort, and may even require relaxation of aviation code.

3. Adverse effects on civil fuel efficiency from a warmer climate

Aviation fuel efficiency is underpinning recent contest between aviation engine makers—using higher bypass engines and improving higher fuel-burning temperature. Aside from technical challenges, further improvements in fuel-burning efficiency may also have safety consequences. In the following discussion, a normal seven-stage flight profile (these are A, start and taxi to runway; B, takeoff and initial climbing; C, climbing to cruising altitude; D, en route cruising; E, descent; F, approach (includes ~8-minute holding at ~1500 ft. approach and landing); and G, taxi to docking) is considered (**Figure 5**). **Figure 5** also shows the typical fuel-burning rates at different stages of a commercial airplane engine.

In this subsection, we start from the theoretical expression of the total work an aircraft needs to perform from the origin airport to the destination airport. Another aspect of the fuel efficiency issue is related to the second law of thermodynamics. All airplane engines are thermal engine. Increased environmental temperature always is detrimental for thermal efficiency. This is directly related to the fuel costs of civil aviation. With changed atmospheric thermal structure, the aircraft's mechanical efficiency may also vary; suppose the same FAA regulation is in position. All components that are sensitive to climate change are investigated and quantitatively from climate model simulations under the RCP 4.5 emission scenario—a more likely scenario.

3.1 Methods and data

During different stages of flying, the force balance situation on an aircraft is different. At the takeoff and climbing stages, there are vertical and forward accelerations. The vertical component of thrust aids the lift in overwhelming gravity. Similarly, the horizontal component of thrust also overwhelms drag. At cruising
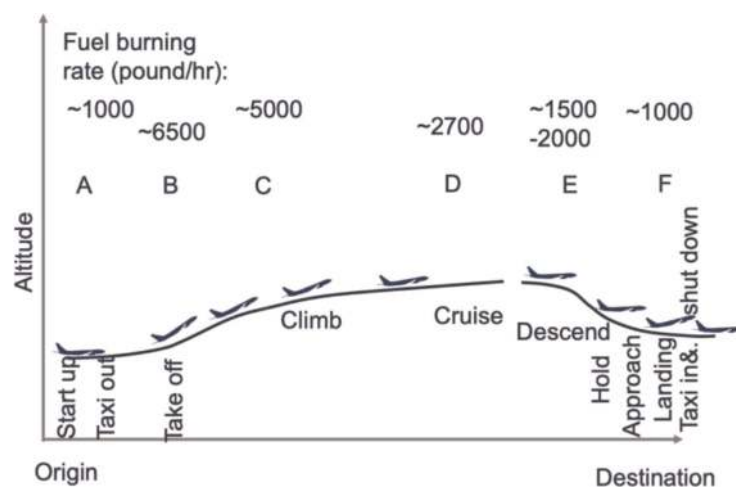
Figure 5.
Typical flight profile of an aircraft and the fuel-burning rate in each stage. Except the cruising stage, other six stages last from 10 to 40 minutes only. In all, cruising stage is the most fuel-consuming stage.

stage, thrust is reduced mainly to counteract drag, and the weight is balanced primarily by lift. Inevitable work done to the aircraft involves lifting it to the cruise elevation. The potential energy cannot be reclaimed at descending stage, unlike electronics cars. This portion of energy only is sensitive to warming when tropopause height changes as climate warms. The far larger term in energy cost would be that used to overcome drag. While it is apparent that drag is proportional to fuel cost, the picture for how total drag is affected by climate change is more sophisticated, because of the multiple sources involved. Classifying the many drag terms into pressure drag (e.g., induced drag, wave drag, and form drag) and skin friction drag (second term on right-hand side of Eq. (3)) is convenient because the pressure drags tend to be proportionally affected by air temperature and density changes. For example, for a specific design, the effects from environmental air on induced drag and net lift are usually proportional. Thus, the changes in skin friction are decisive for the sign of extra drag on top of total drag stress. To separate out climate change effects on aviation, it is assumed that there is no technological advance in design of subsonic aircrafts used for commercial airliners during the timespan of consideration:

$$F_d = \iint\limits_S (p - p^*) \hat{n} \hat{i} dA + \iint\limits_S \tau \hat{t} \hat{i} dA \qquad (3)$$

where F_d is the total drag, $\hat{n}$ and $\hat{t}$ are, respectively, unit vectors in the direction perpendicular and parallel to the local surface element (dA), p is pressure, and $\hat{i}$ is the flow (drag) direction (align with the aircraft trajectory in **Figure 5**). For a specific type of airplane, the second term on the right-hand side of Eq. (3) can be parameterized as $p^* S c_1 R_e^{c_2}$, where S is wing area and R_e is Reynolds' number. Coefficients c_1 (~0.074 for well-painted un-dented surfaces) and c_2 (approximately -0.2) are aircraft dependent. The drag coefficient is inversely related to the Reynolds number. Increased flow speed tends to increase R_e, while increased temperature, with consequently increased dynamic viscosity, tends to reduce R_e. Without resorting to strict model calculation, it is difficult to estimate accurately the net effect from climate warming to total drag.

To have an estimate of the effects by the end of the twenty-first century, we followed a line-by-line analysis of available commercial airliners. For this purpose, online commercial ticketing databases are browsed for available flights among global airports. Non-direct flights are decomposed to several "direct flights" in a row. An annual, global, direct flight database is thus archived for this research. To estimate the total annual fuel consumption, we follow a line-by-line adding method that considers all available (in operation as of 2010) commercial airliners and their scheduled flights. The integration is along the flying trajectory. There are all sorts of alliances and partnerships between the commercial airliners. A trip involving multiple stops is likely carried out by different airliners in collaboration. For example, between Beijing and Singapore, there are 14 companies having such a transportation service at sub-weekly frequency. Asiana and Air China, for example, have a service to take passengers to Seoul first before heading to Singapore. Cathay Pacific and Thai Airlines stop, respectively, in Hong Kong and Bangkok. Xiamen Airlines even make two stops in between (Beijing → Zhoushan → Xiamen → Singapore). To eliminate possible recounting of the flying legs, only direct flights (each involves one takeoff, cruise, and one landing) between airports are analyzed. In the above case between Beijing and Singapore, there are only five such daily flights, from Air China (A975 and A976, Airbus 330 s) and Singapore Airlines (SA801, 805, Boeing 777 s as carrier, and SA 807, an Airbus 380-800). Connecting flights from the same

airline or from several partner airlines are considered to be several connected direct flights, with distinct flight profile legs and usually carried out using different types of aircraft. For example, the Xiamen Airline schedule from Beijing to Singapore is looked upon as a direct flight from Beijing to Zhoushan, followed by a direct flight from Zhoushan to Xiamen, and another direct flight from Xiamen to Singapore. In this specific case, the same types of aircrafts are used. However, for intercontinental flights, usually different types of aircrafts are involved and intercontinental legs cruise at a higher elevation than the domestic legs of flights.

In the estimation of fuel efficiency change by the end of this century, atmospheric parameters (i.e., air temperature and humidity) from multiple climate models (all under RCP 8.5 scenario) are used to drive expressions (Eqs. (3)–(5)), weighted by airplane-specific aerodynamic parameters. Ensemble averages are taken after the along trajectory integrations driven, respectively, by all climate models (**Table 1**). The climate model outputs are obtained from the IPCC Deutsches Klimarechenzentrum (DKRZ) Data Distribution Centre (http://www.ipcc-data.org/sim/gcm_monthly/AR5/Reference-Archive.html). For models providing multiple perturbation runs, only $r1i1p1$ runs are used. There still is quite a large uncertainty with emission scenario. The results presented here thus should not be taken too literally. Instead, its values primarily are quantitatively accurate.

3.2 Results

From the discussion in Section 3.1, we see that the total energy an aircraft needs to perform is the one overcoming the drag force (Eq. (3)) and the one overcoming gravity to the cruising altitude. The drag forces do work all stages taking off and before landing (all the suspension stages), whereas the potential energy increases only during the taking off and climbing to the cruising altitude (usually tropopause elevation for best visibility and thermal efficiency—to be discussed soon). Because the cruising stage is of very different lengths, in the following discussion, we estimate the percentage change in energy (fuel) costs relative to each stage in the A-G profile against their respective values (e.g., changes in fuel cost in each flight stage, rather than vaguely relative to the total seven stages).

3.2.1 Fluctuation of the tropopause height

From **Figure 6**, tropopause has apparent latitudinal distribution: reaching lower pressure (higher altitudes) at the tropical region and drops to higher pressure levels at the polar regions. As climate warms, tropopause was lifted to higher elevations (**Figures 6b** and **7a** and **b**), except very localized regions around the South Pole. This is in agreement with Refs. [20, 21]. Different emission scenarios differ primarily in magnitudes, with decreasing regions totally disappeared for the strong emission scenario RCP 8.5. For the bustling North Atlantic Corridor (NAC, 305–350E; 30–60N), not only the trend but even the differences between the two scenarios (**Figure 7c**) pass a t-test with 95% confidence interval. The tropopause altitude increase rate reaches 6 m/year for a weak emission scenario (RCP 4.5). This is about 4% increase in the fuel cost at the ascending stage for normal commercial flights.

In the ascending stage, (in the vertical direction) the aircraft not only overcomes gravity, but it also experiences drag (both terms in Eq. (3)). As a result, the ascending at the lower altitudes is more fuel-consuming, because of the higher air density. As a result of this fact, the elevated tropopause elevation is only an increase of less than 0.2% in fuel costs for long-range international flights. Except for very short-range flights, the cruising stage is the most fuel-consuming stage. Factors
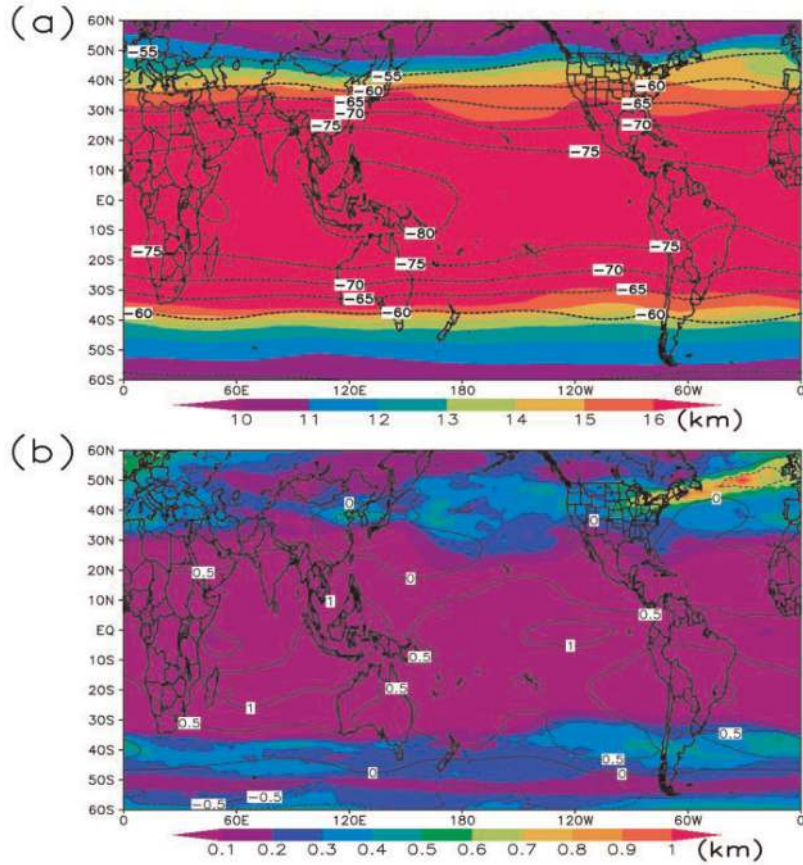
Figure 6.
GFDL2.1 simulated tropopause height (shades in (a), in km) and tropopause temperature (contour lines in (a)) during a control period (1980–2000). The projected differences between (2080–2100) and the control period, under the RCP 8.5 emission scenario, are shown in (b). The increases in tropopause height are a global phenomenon. For most areas, tropopause temperatures also increase.

affecting the cruising stage needed to be examined to have an estimate of the fuel efficiency issue of climate warming.

3.2.2 Thermal, mechanical, and total efficiency

Aircraft engines are breathing thermal engines. That is, they use oxygen in the environmental air fanned into the burning chamber, rather than carrying the oxidizers (as rocket engines do) for burning the fuel. The working fluid is the high-temperature and thus high-pressure exhausts (gases resulting from burning of fuel plus other components in the inhaled air). As fuel and inhaled air are "locked" in the burning chamber moving with the aircraft, the overall efficiency (in providing thrust) is a multiplication of thermal efficiency and mechanical efficiency. Applying Newton's third law of motion (or momentum theory) $F\Delta t = m\Delta V$, it is straightforward to ascertain that the overall efficiency, η, is the multiplication of mechanical efficiency (η_M) and thermal efficiency (η_T), or $\eta = \eta_M \times \eta_T$ (e.g., Ref. [22]).

As aircraft engines are thermal engines, their thermal efficiency is adversely affected by environmental temperature rise. The second law of thermodynamics puts a fundamental limit on thermal efficiency (η_T):

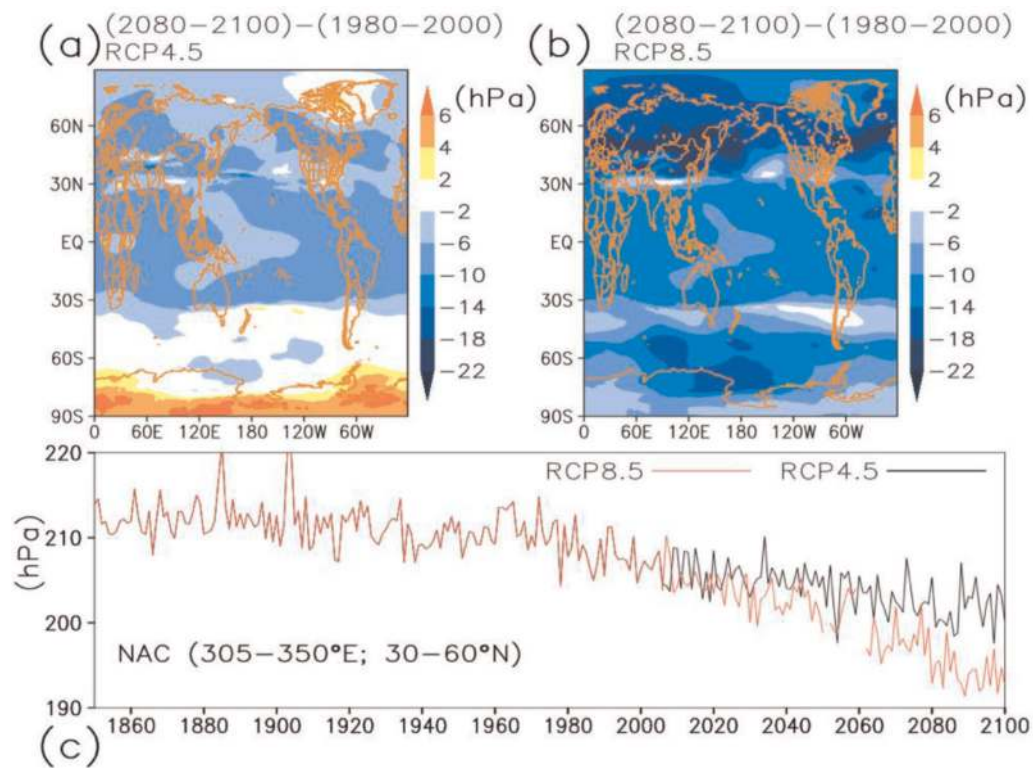$$\eta_T = \varepsilon(1 - T_C/T_H) \tag{4}$$

Figure 7.
GFDL2.1 simulated tropopause height changes (shades in (a) and (b), in hPa) between periods 1980–2000 and 2080–2100, represented in pressure levels. The area averaged time series over the NAC (305–350E; 30–60N) is shown in (c), for two emission scenarios (RCP 4.5 and RCP 8.5). The two differs only quantitatively.

where ε is a technical limiting factor ($\sim$0.57) indicating actual engines' closeness to ideal engine [9], T_H is the absolute temperature at which the heat enters the engine cycle (also called turbine entry temperatures, TETs), and T_c is the absolute temperature of the exhaust gases. T_c closely follows the environmental air temperature, T_a, with only a cooling technology-dependent constant difference. The efficiency of thermal engines increases with higher operating temperature and lower environmental temperature. There have been active efforts in improving TETs during the past 50 years (Section 7.4.1.2 of IPCC AR5: aviation and the global atmosphere). In this study, for simplicity, we assume that both T_H and ε are not going to improve in the projection period (between 2010 and 2100). T_c is the only variable being considered varying along the cruising route. For all commercial brands in operation, the TETs published during 2010–2014 are used. Except for several well-known engine types, most engine companies are very protective of actual engine data and operating conditions, although there is much discussion in the literature and also clues such as in EASA (and FAA) type of certificates (certificates for all of the engine types are publicly available), which have detailed listings of actual engine values in regions where engine measurements are made. The TETs can be deduced from the emission data. According to Eq. (4), a decrease in thermal efficiency for common commercial engines, GE90, RB211, LAEV2500, and Lyulka, in response to a 1 K increase in environmental temperature (T_c), are, respectively, 5.62×10^{-4}, 5.88×10^{-4}, 5.07×10^{-4}, and 4.94×10^{-4}. The effects on engine thermal efficiency from climate change are transferred to the air temperature variations along the flying routes (legs). As the oxygen is inhaled from environmental air (common to breathing engines), and the density decrease due to climate warming does not result in incrementing oxygen concentration in the

environmental air (as a matter of fact, if vapor content is considered, a decrease in oxygen concentration is expected), a natural consequence is that this may result in incomplete fuel oxidization, without technological improvements to the combustion system to increase the volumetric air inhaling rate. This detrimental effect on thrust production is not considered here but is apparently proportional to air density decrease.

As the airplane moves forward by ejecting exhausts backward, the way in which the kinetic energy (extracted from the fuel-burning chemical energy) is partitioned between aircraft and exhaust jet (i.e., used for pushing aircraft forward versus removed by the exhaust) is measured by the mechanical (propulsive) efficiency (η_M):

$$\eta_M = \frac{2}{1 + V_e/V_a} \tag{5}$$

where V_e is effective exhaust speed (jet speed relative to airplane) and the airplane speed, V_a, is relative to the ground. η_M reaches maximum when the jet exhaust is stationary relative to the ground (all extracted energy from fuel burning is used as thrust to push forward the aircraft). Here exhaust speed is retrieved from TETs and engine pressure ratios [23]. Equation (5) is derived in the inertial frame coordinates based on energy and momentum conservation. The commercial passenger aircrafts generally have effective jet speeds, V_e, within the range of 600–850 m/s. The lower the effective jet speed (i.e., close to the cruising speed), the more sensitive the mechanical efficiency is to airplane cruising speeds. Overall efficiency η is the multiplication of mechanical efficiency and thermal efficiency ($\eta = \eta_M \times \eta_T$). Factors lowering (enhancing) overall efficiency result in more (less) fuel cost.

In the global belt between 65°S and 70°N, which contains most of the trajectories of commercial flights, the tropopause temperature increased ~0.8–1.2°C over a 100-year period (the difference between (2080–2100) and (1980–2000)). For most commercial engines, thermal efficiency reduces only 0.06% during the cruising stage of the flight profile. Due to air density decrease, the mechanical efficiency is affected by warming the opposite way. As a result, the total efficiency was affected only by ~0.03%. The most significant effect from a warming flying environment is in fact from the increased air stickiness—the body drag acting on the aircraft.

3.2.3 Drag on aircraft

The percentage change in skin friction drag is caused primarily by the increase in the kinematic viscosity of air, within the cruising space, which has a temperature lapse rate of about 8×10^{-8} m^2 s^{-1} K^{-1}. **Figure 8c** indicates that, for all operating airliners considered, there could be a 3.5% increase in skin frictional drag by 2100 ($\Delta\tau/\tau^0 = 0.035$, with superscript means the value at reference year 2010), whereas the skin friction drag is only ~5.7% of the total drag. The increase in skin frictional drag accounts only for a ~0.2% reduction in efficiency in fuel consumption. Thus, due to increased air viscosity and decreased engine overall efficiency, the annual fuel consumption in 2100 would be ~0.9% higher than around 2010. The spread in the estimation is wide among climate models, but all indicate more fuel consumption as climate warms. The corresponding absolute change of 0.9% reduction in efficiency in fuel consumption is considerable, about 0.68 billion gallons of fuel annually. The reduction in thermal efficiency is complementary to the IPCC AR5 perspective, but the fact that the increased drag and mechanical efficiency may be a supplant concept (a new rubric) will hopefully stimulate further studies in this
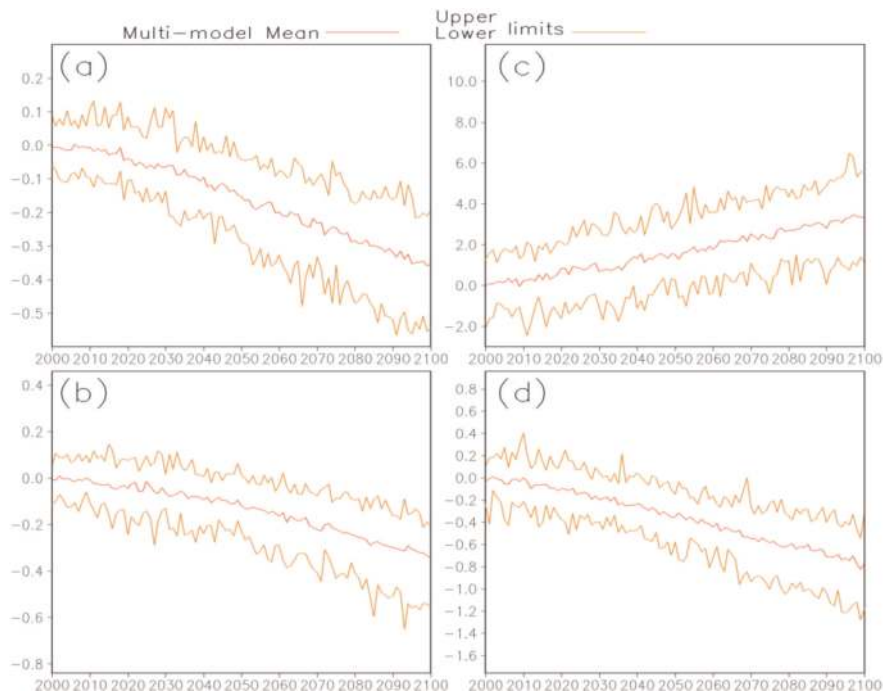
Figure 8.
Decreases in thermal efficiency (a) and mechanical efficiency (b), increase in skin frictional drag (c), and the overall decrease in fuel efficiency (d) during 2000–2100, for entire commercial aviation sector as a whole. Multiple climate model ensemble means (shown as thick red lines), and the ranges of the variability (thick yellow lines) are shown for 24 climate models under RCP 8.5 emission scenarios (for clarity only, the other two models both are within the range). The flight schedules of year 2010 are assumed unchanged during the entire period. Note that the control period is centered on 2010 (2005–2015), so the values at starting (2000) is not exactly united.

direction. A *t*-test was performed for the overall decrease in fuel efficiency time series. For 22-year periods centered at year 2010 and 2090, a *P*-value of 0.0017 (*dof* = 38) was obtained. At this significant level, it means at a possibility of 99.84%, the trend is not by mere coincidence. Thus, the net decrease in fuel efficiency is small but statistically significant.

3.3 Conclusion

To conclude, factors affecting aviation fuel efficiency are thermal and propulsive efficiencies and overall drag on aircrafts. An along-the-route integration is made for all direct flights in baseline year 2010, under current and future atmospheric conditions from nine climate models under the representative concentration pathway (RCP) 8.5 scenario. Thermal and propulsive efficiencies are affected oppositely by environmental warming. The former decreases 0.38%, but the latter increases 0.35% over the twenty-first century. Consequently, the overall engine efficiency decreases only by 0.02%. Over the same period, skin frictional drag increases ~5.5%, from the increased air stickiness. This component is only 5.7% of the total drag, the ~5.5% increase in air viscosity accounts for a 0.275% inefficiency in fuel consumption, one order of magnitude larger than that caused by engine efficiency reduction. The total decrease in fuel efficiency equals to ~0.24 billion gallons of extra fuel annually, a qualitatively robust conclusion but quantitatively with significantly inter-climate model spread.

The effects on fuel cost from increased airplane potential energy still is one order of magnitude smaller than factors considered here, due to the fact that it is a less than a 1% increase in the climbing stage (at most 1 hour). The fuel cost, in the

cruising stage is much greater, because of the length of time (up to 14 hours). Also, at higher altitudes, the fuel cost for climbing is reduced (the increased tropopause height's effect is the upper level part of the trajectory). The common statement that the climb stage is more fuel-consuming refers to the rate, not the total value (except for very short flights, e.g., from Oklahoma City to Tulsa).

Climate effects on aviation are a burgeoning but promising research field. Our study here focused on the rudimentary aspects that are of concern to the commercial airlines: the effects on maximum payload and on fuel costs. Other directions such as customer comfort and safety also are profoundly affected, especially the circulation changes (winds and turbulence [24]). These will be addressed in future studies in this walk of line.

Acknowledgements

Conflict of interest

The authors claim no conflict of interest in this research.

Author details

Diandong Ren[1] and Lance M. Leslie[2]*

1 Curtin University, Perth, Australia

2 University Technology, Sydney, Australia

*Address all correspondence to: lmleslie@ou.edu

IntechOpen

References

[1] Minnis P et al. Global distribution of contrail radiative forcing. Geophysical Research Letters. 1999;**26**:1853-1856

[2] IPCC. Understanding the Climate System and its Recent Changes. In: Summary for Policymakers. IPCC AR5 WG1; 2013

[3] IPCC. Aviation and the Global Atmosphere—A Summary for Policy Makers. UK: Cambridge University Press; 1999. p. 373

[4] Sausen R et al. Aviation radiative forcing in 2000: An update on IPCC (1999). Meteorologische Zeitschrift. 2005;**14**:555-561

[5] Fichter C, Marquart S, Sausen R, Lee D. The impact of cruise altitude on contrails and related radiative forcing. Meteorologische Zeitschrift. 2005;**14**: 563-572

[6] Fu Q, Liou KJ. Parameterization of the radiative properties of cirrus clouds. Atmospheric Sciences. 1993;**50**: 2008-2025

[7] Stuber N, Forster P, Radel G, Shine K. The importance of the diurnal and annual cycle of air traffic for contrail radiative forcing. Nature. 2006;**441**: 864-867

[8] Lewis S, Karoly D. Are estimates of anthropogenic and natural influences on Australia's extreme 2010–2012 rainfall model-dependent? Climate Dynamics. 2015;**45**:679-695

[9] Holman J. Thermodynamics. New York: McGraw-Hill; 1980. p. 217

[10] Wallace J, Hobbs P. Atmospheric Science. 2nd ed. Burlington, MA, USA: Academic Press; 2006. p. 504

[11] Taylor K, Stouffer R, Meehl G. An overview of CMIP5 and the experiment design. Bulletin of the American Meteorological Society. 2012;**93**:485-498

[12] Kistler R et al. The NCEP–NCAR 50-year reanalysis: Monthly means CD-ROM and documentation. Bulletin of the American Meteorological Society. 2001;**82**:247-267

[13] Lawrence M. The relationship between relative humidity and the dew point temperature in moist air: A simple conversion and applications. Bulletin of the American Meteorological Society. 2005;**86**:225-233

[14] Trenberth K. Changes in precipitation with climate change. Climate Research. 2011;**47**:123-138

[15] Allen M, Ingram W. Constraints on future changes in climate and the hydrologic cycle. Nature. 2002;**419**: 224-232

[16] Held I, Soden B. Robust response of the hydrological cycle to global warming. Journal of Climate. 2006;**19**: 5686-5699

[17] Khon V et al. Response of the hydrological cycle to orbital and greenhouse gas forcing. Geophysical Research Letters. 2010;**37**:L19705

[18] Coffel E, Horton R. Climate change and the impact of extreme temperatures on aviation. Weather, Climate, and Society. 2015;**7**:94-102

[19] Hane F. Comment on "climate change and the impact on extreme temperatures on aviation". Weather, Climate, and Society. 2016;**8**:205-206

[20] Santer B et al. Behavior of tropopause height and atmospheric temperature in models, reanalyses, and observations: Decadal changes. Journal of Geophysical Research. 2003;**108**(D1): 4002. DOI: 10.1029/2002JD002258

[21] Reichler T, Martin D, Sausen R. Determining the tropopause height from gridded data. Geophysical Research Letters. 2003;**30**:2042. DOI: 10.1029/2003GL018240

[22] Kershner W. The Advanced Pilot's Flight Manual, 392. 8th ed. Newcastle, WA, USA: Aviation Supplies and Academics, Inc; 2015

[23] Cumpsty NA. Jet Propulsion. Cambridge, United Kingdom and New York, NY, USA: Cambridge University Press; 1997

[24] Ren D. Effects of global warming on wind energy availability. Journal of Renewable and Sustainable Energy. 2010;**2**:052301. DOI: 10.1063/1.3486072